Available online at www.sciencedirect.com
SCIENCE DIRECT®
Surface Science 583 (2005) 213–228
SURFACE SCIENCE
www.elsevier.com/locate/susc

A new theoretical approach to multilayer adsorption of polyatomics

F. Romá, A.J. Ramirez-Pastor *, J.L. Riccardo

Departamento de Física, Universidad Nacional de San Luis—CONICET, Chacabuco 917, 5700 San Luis, Argentina

Received 29 October 2004; accepted for publication 8 February 2005
Available online 13 April 2005

Abstract

The multilayer adsorption isotherms of linear particles (k-mers) on homogeneous surfaces were developed on a generalization in the spirit of the well-known Brunauer–Emmet–Teller's approach. The generalized equation is obtained through an analytical approach that provides the isotherm in the multilayer regime from the isotherm in the monolayer regime. The formalism leads to exact results in one dimension and provides an analytical approximation to study multilayer adsorption on two-dimensional surfaces with different geometries (square, honeycomb and triangular). The entropic effects of the nonspherical character of the adparticles on the determination of the monolayer volume and adsorption energy, are shown and discussed for type II and type III isotherms. Comparison with Monte Carlo simulations in the grand canonical ensemble and experimental adsorption isotherms are used to test the accuracy and reliability of the model. Close agreement between simulated, theoretical and experimental results supports the applicability of the proposed model to describe multilayer adsorption in presence of multisite-occupancy.

Keywords: Monte Carlo simulations; Equilibrium thermodynamics and statistical mechanics; Surface thermodynamics; Adsorption isotherms

1. Introduction

Multilayer adsorption has been attracting a great deal of interest since long ago [1–4] and the progress in this field has gained a particular impetus due to its importance for the characterization of solid surfaces. Various theories have been proposed to describe multilayer adsorption in equilibrium [5–9]. Among them, the Brunauer–Emmet–Teller (BET) model [9] is one of the most widely used and practically applicable. The great popularity of the BET equation in experimental studies of adsorption has led some authors to

* Corresponding author. Tel.: +54 2652 536151; fax: +54 2652 430224.
E-mail address: antorami@unsl.edu.ar (A.J. Ramirez-Pastor).

0039-6028/$ - see front matter © 2005 Elsevier B.V. All rights reserved.
doi:10.1016/j.susc.2005.02.058

extend the original theory of multilayer adsorption. Thus, numerous generalizations of the BET model have been reported in the literature, including surface heterogeneity, lateral interaction between the admolecules, differences between the adsorption energy and structure between the first and upper layers, etc., [2,4]. These leading models, along with much recent contributions, have played a central role in the characterization of solid surfaces by means of gas adsorption [10]. One fundamental feature of BET's model is preserved in all these theories. This is the assumption that an adsorbed molecule occupies one adsorption site.

In practical situations, most adsorbates involved in adsorption experiments are polyatomic in the sense that, when adsorbed, their typical size is larger than the distance between the nearest-neighbor local minima of the gas–solid potential. For instance, this is true for most *n*-alkanes [3], *n*-alkenes, cyclic hydrocarbons, etc. However, even the simplest nonspherical molecules such as N_2 and O_2 may adsorb on more than one site depending on the surface structure [11–17]. This effect, so-called multisite occupancy adsorption, introduces a high degree of difficulty in the adsorption theories. Consequently, a few elaborated analytical isotherms [10,18–29] and numerical studies [30–37] have been derived for describing the peculiarities of polyatomics adsorption.

Hence, a more accurate description of multilayer adsorption should account for the fact that it develops in general with multisite occupancy. Although many other factors have been considered in multilayer adsorption, there have been a few studies accounting for the fact of multiple occupation of sites at multilayer regime [38–40]. Thus, in Refs. [38,39], Aranovich and Donohue presented a multilayer adsorption isotherm, which is not limited by the functional form of the monolayer adsorption isotherm and should be capable to include multisite occupancy (with an adequate choice of a fitting parameter). On the other hand, the closed exact solution for the multilayer adsorption isotherm of dimers, along with the basis for calculating adsorption thermodynamics of homonuclear polyatomic molecules (*k*-mers) on one-dimensional substrates, have been recently presented [40]. This rigorous thermodynamic study demonstrated that the entropic contribution of nonspherical adsorbates is significant in the multilayer regime when compared with monoatomic adsorption. Thus, the determinations of surface areas and adsorption energies from polyatomic adsorbate adsorption may be severely misestimated, if this polyatomic character is not properly incorporated in the thermodynamic functions from which experiments are interpreted.

In this context, the aim of the present work is to extend the treatment of Ref. [40] to include the two-dimensional nature of the substrate. For this purpose, a new theoretical formalism is presented based upon (i) the analytical expression of the adsorption isotherm at monolayer and (ii) a mapping from the grand partition function of the monolayer to the grand function of partition of the multilayer, where the fugacity of the monolayer transforms into the grand partition function of a single column of *k*-mers. In addition, Monte Carlo (MC) simulations are performed in order to test the validity of the theoretical model. The new theoretical scheme allows us: (1) to reproduce the well-known BET isotherm for monomers [9] and the exact dimer isotherm presented in [40]; (2) to develop a closed exact expression for the multilayer adsorption isotherm of *k*-mers on one dimension; (3) to obtain an accurate approximation for multilayer adsorption on two-dimensional substrates accounting multisite occupancy and (4) to provide a simple model from which experiments may be reinterpreted.

The present work is organized as follows. In Section 2, the theoretical formalism is presented. In Section 3, the basis of the MC method are given. In Section 4, the results of the theoretical model are shown and discussed by comparing with experimental data and MC simulations. Finally, conclusions are drawn in Section 5.

2. Theory

In order to maintain the simplest model that accounts for multisite-occupancy in multilayers we define it in the spirit of the BET's original formulation. The adsorbent is a homogeneous lattice of sites. The adsorbate is assumed as linear molecules

having k-identical units (k-mers) each of which occupies an adsorption site. The concept of linear k-mer is trivial for square and triangular lattices [see Fig. 1(a) and (b), respectively]. However, in a honeycomb lattice, the geometry does not allow the existence of a linear array of monomers. In this case, we call linear k-mer to a chain of adjacent monomers with the following sequence: once the first monomer is in place, the second monomer occupies one of the three nearest-neighbor of the first monomer. Third monomer occupies one of the two nearest-neighbor of the second monomer. i-esime monomer (for $i \geqslant 4$) occupies one of the two nearest-neighbor of the preceding monomer, which maximizes the distance between first monomer and i-esime monomer. This procedure allow us to place k monomers on a honeycomb lattice without creating an overlap. As an example, Fig. 1(c) shows a available configuration for a linear tetramer adsorbed on a honeycomb lattice. Once first, second and third monomers were adsorbed in positions denoted as a, b and c, respectively, there exist two possible positions for adsorbing fourth monomer, d and e. In order to maximize the distance between the position of first and fourth monomers, site d is selected and site e is discarded. Furthermore, (i) a k-mer can adsorb exactly onto an already adsorbed one; (ii) no lateral interactions are considered; (iii) the adsorption heat in all layers, except the first one, equals the molar heat of condensation of the adsorbate in bulk liquid phase. Thus, $c = q_1/q_i = q_1/q$ with $q_i = q$ ($i = 2, \ldots, \infty$) denotes the ratio between the single-molecule partition functions in the first and higher layers. The fact that k-mers can arrange in the first layer leaving sequences of l empty sites

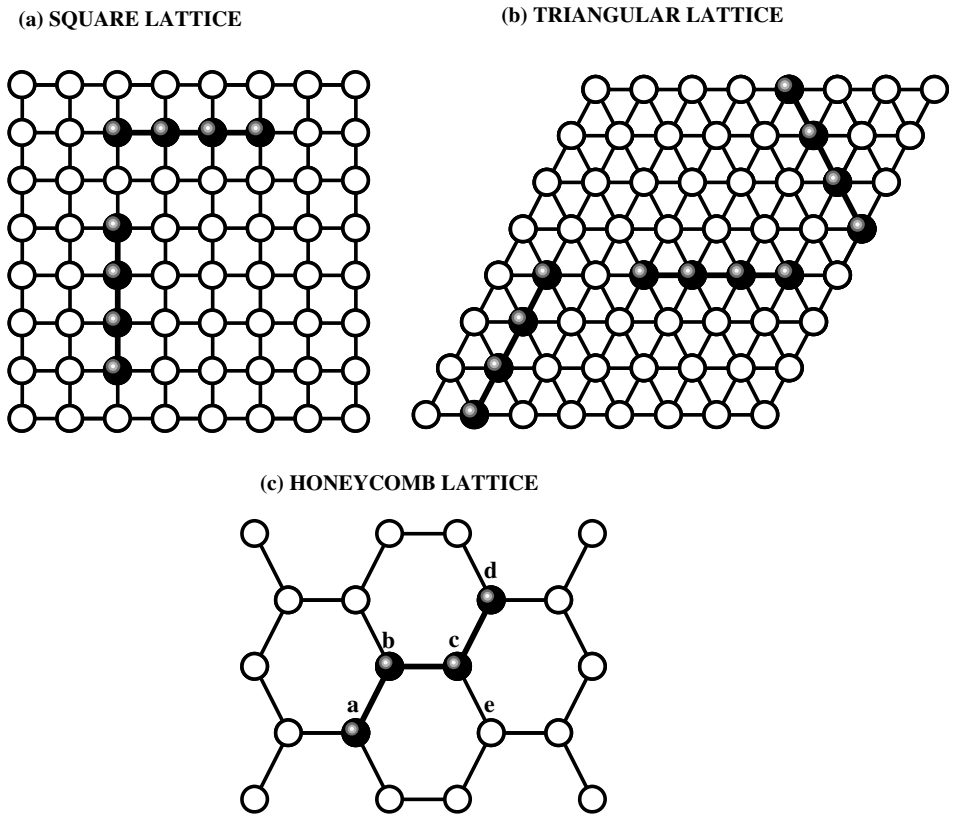

Fig. 1. Linear tetramers adsorbed on (a) square, (b) triangular and (c) honeycomb lattices. Full and empty circles represent tetramer units and empty sites, respectively.

with $l < k$, where no further adsorption of a k-mer can occur in such a configuration, makes the calculation of entropy much elaborated than the one for monomer adsorption.

For a lattice having M adsorption sites, the maximum number of columns that can be grown up onto it is $n_{\max} = M/k$. Let us denote by $\Omega_k(n, M)$ the total number of distinguishable configurations of n columns on M sites. If an infinite number of layers is allowed to develop on the surface, the grand partition function, Ξ_{mul}, of the adlayer in equilibrium with a gas phase at chemical potential μ and temperature T, is given by

$$\Xi_{\mathrm{mul}} = \sum_{n=0}^{n_{\max}} \Omega_k(n, M)\xi^n, \tag{1}$$

where ξ is the grand partition function of a single column of k-mers having at least one k-mer in the first layer. Then,

$$\xi = \sum_{i=1}^{\infty} q_1 q^{i-1} \lambda_{\mathrm{mul}}^i = c \sum_{i=1}^{\infty} q^i \lambda_{\mathrm{mul}}^i = \frac{c\lambda_{\mathrm{mul}} q}{1 - \lambda_{\mathrm{mul}} q} = \frac{cx}{1-x}, \tag{2}$$

where $\lambda_{\mathrm{mul}} = \exp(\mu/k_{\mathrm{B}}T)$ is the fugacity and k_{B} is the Boltzmann constant. In addition, it is possible to demonstrate that $x = \lambda_{\mathrm{mul}} q = p/p_0$ is the relative pressure [10,40].

On the other hand, the grand partition function of the monolayer, Ξ_{mon}, can be written as

$$\Xi_{\mathrm{mon}} = \sum_{n=0}^{n_{\max}} \Omega_k(n, M)\lambda_{\mathrm{mon}}^n \tag{3}$$

in this case, n represents the number of adsorbed k-mers and λ_{mon} is the monolayer fugacity.

By comparing Eqs. (1) and (3) and from the condition,

$$\lambda_{\mathrm{mon}} = \xi = \frac{cp/p_0}{1 - p/p_0} \Rightarrow \frac{p}{p_0} = \frac{1}{1 + c\lambda_{\mathrm{mon}}^{-1}}, \tag{4}$$

we can write the monolayer coverage, θ_{mon}, as

$$\theta_{\mathrm{mon}} = \frac{k}{M}\tilde{n} = \frac{k}{M}\lambda_{\mathrm{mon}}\left(\frac{\mathrm{d}\ln \Xi_{\mathrm{mon}}}{\mathrm{d}\lambda_{\mathrm{mon}}}\right)_{M,T} = \frac{k}{M}\xi\left(\frac{\mathrm{d}\ln \Xi_{\mathrm{mul}}}{\mathrm{d}\xi}\right)_{M,T}, \tag{5}$$

where n is the mean number of columns. In addition, the total coverage, θ, can be written as

$$\theta = \frac{k}{M}\widetilde{N} = \frac{k}{M}\lambda_{\mathrm{mul}}\left(\frac{\mathrm{d}\ln \Xi_{\mathrm{mul}}}{\mathrm{d}\lambda_{\mathrm{mul}}}\right)_{M,T}, \tag{6}$$

where $\widetilde{N}$ is the mean number of adsorbed k-mers. After some algebra the total coverage can be written in terms of the monolayer coverage,

$$\theta = \frac{k}{M}\lambda_{\mathrm{mul}}\left(\frac{\mathrm{d}\ln \Xi_{\mathrm{mul}}}{\mathrm{d}\xi}\right)_{M,T}\frac{\mathrm{d}\xi}{\mathrm{d}\lambda_{\mathrm{mul}}} = \frac{\theta_{\mathrm{mon}}}{(1 - p/p_0)}. \tag{7}$$

Finally, the theoretical procedure can be described as follows:

(1) By using θ_{mon} as a parameter ($0 \leqslant \theta_{\mathrm{mon}} \leqslant 1$), the relative pressure is obtained by using Eq. (4). This calculation requires the knowledge of an analytical expression for the monolayer adsorption isotherm.
(2) The values of θ_{mon} and p/p_0 are introduced in Eq. (7) and the total coverage is obtained.

The items (1) and (2) are summarized in the following scheme:

$$\theta_{\mathrm{mon}} + \lambda_{\mathrm{mon}}(\theta_{\mathrm{mon}}) + \text{Eq. (4)} \rightarrow p/p_0 \Rightarrow \theta_{\mathrm{mon}} + p/p_0 + \text{Eq. (7)} \rightarrow \theta. \tag{8}$$

3. Monte Carlo simulation of adsorption in the grand canonical ensemble

Following the Metropolis scheme [41], the transition probability from a state i to a new state j, $W(i \rightarrow j)$, is defined by

$$W(i \rightarrow j) = \min\{1, \exp[-\beta(\Delta U - \mu\Delta N)]\}, \tag{9}$$

where $\beta = 1/k_{\mathrm{B}}T$, and ΔN and ΔU represent the variation in the number of particles and the variation in the total energy, respectively, when the system changes from the state i to the state j.

In adsorption–desorption equilibrium there are four elementary ways to perform a change of the system state, namely, adsorbing one molecule onto the surface, desorbing one molecule from the surface, adsorbing one molecule in the higher layers

and desorbing one molecule from the higher layers. The corresponding transition probabilities are,

- $W_{\mathrm{ads}}^{\mathrm{surf}} = \min\{1, \exp[-\beta(U_1 - \mu)]\}$, (10)

where $W_{\mathrm{ads}}^{\mathrm{surf}}$ is the transition probability of adsorbing one molecule onto the surface and U_1 is adsorption energy of one molecule on the surface. In addition, $\exp[-\beta(U_1-\mu)] = q_1\lambda$, $q_1 = cq$ and $q\lambda = p/p_0$. Then,

$$W_{\mathrm{ads}}^{\mathrm{surf}} = \min\left\{1, c\frac{p}{p_0}\right\}, \tag{11}$$

- $W_{\mathrm{des}}^{\mathrm{surf}} = \min\{1, \exp[\beta(U_1 - \mu)]\}$, (12)

where $W_{\mathrm{des}}^{\mathrm{surf}}$ is the transition probability of desorbing one molecule from the surface, which can be written in terms of p/p_0 as

$$W_{\mathrm{des}}^{\mathrm{surf}} = \min\left\{1, \frac{1}{c}\frac{p_0}{p}\right\}, \tag{13}$$

- $W_{\mathrm{ads}}^{\mathrm{bulk}} = \min\{1, \exp[-\beta(U - \mu)]\}$, (14)

where $W_{\mathrm{ads}}^{\mathrm{bulk}}$ is the transition probability of adsorbing one molecule in the bulk liquid phase and U is adsorption energy of one molecule on the ith layer with $i \geqslant 2$. In addition, $\exp[-\beta(U-\mu)] = q\lambda = p/p_0$. Then,

$$W_{\mathrm{ads}}^{\mathrm{bulk}} = \min\left\{1, \frac{p}{p_0}\right\}, \tag{15}$$

- $W_{\mathrm{des}}^{\mathrm{bulk}} = \min\{1, \exp[\beta(U - \mu)]\}$, (16)

where $W_{\mathrm{des}}^{\mathrm{bulk}}$ is the transition probability of desorbing one molecule from the bulk liquid phase. Then,

$$W_{\mathrm{des}}^{\mathrm{bulk}} = \min\left\{1, \frac{p_0}{p}\right\}. \tag{17}$$

The algorithm to carry out an elementary step in MC simulation (1 *MCS*), is the following:

(1) Set the value of the relative pressure p/p_0 and the temperature T.
(2) Set an initial state by adsorbing N molecules in the system. Each k-mer can adsorb in two different ways: (i) on a linear array of (k) empty sites on the surface or (ii) exactly onto an already adsorbed k-mer.
(3) Introduce an array, denoted as A, storing the coordinates of n_{e} entities, being n_{e},

$$\begin{aligned} n_{\mathrm{e}} = {} & \text{number of available adsorbed} \\ & k\text{-mers for desorption } (n_{\mathrm{d}}) \\ & + \text{number of available} \\ & k\text{-uples for adsorption } (n_{\mathrm{a}}), \end{aligned} \tag{18}$$

where n_{a} is the sum of two terms: (i) the number of k-uples of empty sites on the surface and (ii) the number of columns of adsorbed k-mers.[1]
(4) Choose randomly one of the n_{e} entities, and generate a random number $\kappa \in [0, 1]$
  (4.1) if the selected entity is a k-uple of empty sites on the surface then adsorb a k-mer if $\kappa \leqslant W_{\mathrm{ads}}^{\mathrm{surf}}$.
  (4.2) if the selected entity is a k-uple of empty sites on the top of a column with i k-mers then adsorb a new k-mer in the $i+1$ layer if $\kappa \leqslant W_{\mathrm{ads}}^{\mathrm{bulk}}$.
  (4.3) if the selected entity is a k-mer on the surface then desorb the k-mer if $\kappa \leqslant W_{\mathrm{des}}^{\mathrm{surf}}$.
  (4.4) if the selected entity is a k-mer on the top of a column then desorb the k-mer if $\kappa \leqslant W_{\mathrm{des}}^{\mathrm{bulk}}$.
(5) If an adsorption (desorption) is accepted in (4), then, the array A is updated.
(6) Repeat from step (4) M times.

In the present case, the equilibrium state could be well reproduced after discarding the first $m \approx 10^4$ *MCS*. Then, averages were taken over $m' \approx 10^4$ *MCS* successive configurations. The total coverage was obtained as simple averages,

$$\theta = \frac{k\langle N\rangle}{M}, \tag{19}$$

where $\langle N\rangle$ is the mean number of adsorbed particles, and $\langle\cdots\rangle$ means the time average over the MC simulation runs.

[1] Note that the top of each column is an available k-uple for the adsorption of one k-mer.

4. Results

4.1. Exact solution in 1-D

By following the scheme presented in the previous section, we can obtain the exact solution for multilayer adsorption of k-mers on a one-dimensional lattice.

We start from the equation

$$\lambda_{\mathrm{mon}} = \frac{\theta_{\mathrm{mon}}}{k} \frac{\left[1 - \dfrac{(k-1)}{k}\theta_{\mathrm{mon}}\right]^{k-1}}{(1-\theta_{\mathrm{mon}})^{k}}, \tag{20}$$

which represents the one-dimensional exact isotherm of k-mers adsorbed at monolayer [26].

Substituting Eq. (20) into Eq. (4), one obtains the following expression for the relative pressure,

$$\frac{p}{p_0} = \frac{\theta_{\mathrm{mon}}\left[1 - \dfrac{(k-1)}{k}\theta_{\mathrm{mon}}\right]^{k-1}}{kc(1-\theta_{\mathrm{mon}})^{k} + \theta_{\mathrm{mon}}\left[1 - \dfrac{(k-1)}{k}\theta_{\mathrm{mon}}\right]^{k-1}}. \tag{21}$$

Eqs. (7) and (21) represent the exact solution describing the adsorption of k-mers at multilayer regime on a homogeneous surface in 1-D. In the case of monomer adsorption ($k = 1$), Eqs. (7) and (21) reduce to the well-known BET isotherm [9], i.e.

$$\theta = \frac{cp/p_0}{(1-p/p_0)[1+(c-1)p/p_0]} \quad k = 1. \tag{22}$$

For $k = 2$, the dimer isotherm can be written in a simple form:

$$\theta = \frac{1}{(1-p/p_0)}\left\{1 - \left[\frac{1-p/p_0}{1+(4c-1)p/p_0}\right]^{1/2}\right\} \quad k = 2. \tag{23}$$

By using other methodology, the Eq. (23) has been recently reported in the literature [40].

In Fig. 2 we address the comparison between the analytical adsorption isotherm in 1-D and MC simulation. The simulations have been performed for monomers, dimers and 10-mers adsorbed on chains of $M/k = 1000$ sites with periodic boundary conditions. Different values of the parameter c have been considered. In all cases, the computational data fully agree with the theoretical predictions, which reinforces the robustness of the two methodologies employed here.

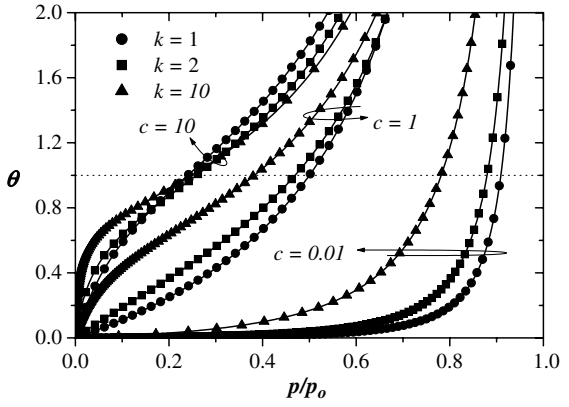

Fig. 2. Adsorption isotherms for k-mers on one-dimensional lattices and different values of the parameter c (as indicated). Solid lines and symbols represent theoretical and simulation results, respectively.

As it can be observed from Fig. 2, for certain values of the parameter c, the corresponding isotherm has a point of inflection. The point of inflection can be obtained in three steps: (1) differentiating twice the adsorption isotherm equation to obtain $\mathrm{d}^2\theta/\mathrm{d}Y^2$ (being $Y = p/p_0$ for the sake of simplicity); (2) equating the resulting expression to zero and solving for Y gives Y_F, the value of p/p_0 at the point of inflection; and (3) inserting Y_F in the adsorption isotherm equation gives θ_F, the value of θ at the point of inflection.

The location of the point of inflection ($X_F \equiv \theta_F, Y_F$) is plotted in Fig. 3 for different values of c and k. Clearly, the value of θ at the point of inflection may deviate considerably from unity. However, there exist a certain value of $c = c_m$, where the point of inflection coincides with the point corresponding to the monolayer capacity. Fig. 4 shows the behavior of c_m as a function of k. The values of c_m, which have been obtained numerically in the range $k = 1$–10, provide a exponential dependence [$\exp(bk)$]. As shown in the inset, $b \approx 0.79$, obtained from the slope of $\ln c_m$ vs. k. For values of c between c_m and infinity the adsorption at the point of inflection exceeds the

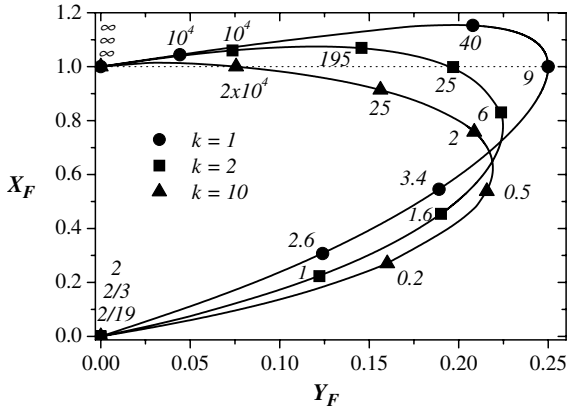

Fig. 3. Coordinates of the point of inflection (being X_F and Y_F coverage and relative pressure, respectively) for one-dimensional adsorption isotherms with different values of k ($k = 1, 2, 10$). Each point (solid circle) in a given curve corresponds to a determined value of c, as indicated.

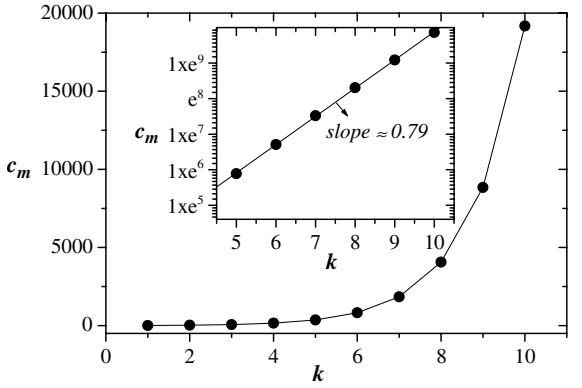

Fig. 4. c_m (as it is indicated in the text) as a function of size of adsorbate, k, for adsorption isotherms of k-mers on one-dimensional lattices.

monolayer capacity; for values of c below c_m the two quantities deviate more and more and for a limit value of $c = c_n$, the point of inflection disappears. c_n vs. k can be calculated analytically (see Appendix A for further discussion). The result of this calculation is presented in Fig. 5. As it is can be visualized from the figure, the function $c_n(k) = 2/(2k - 1)$ separates two well differentiate regions: (i) for $c > c_n$, the isotherm is of Type II and (ii) when c is less than c_n the isotherm is of Type III and discussion of the point of inflection is meaningless.

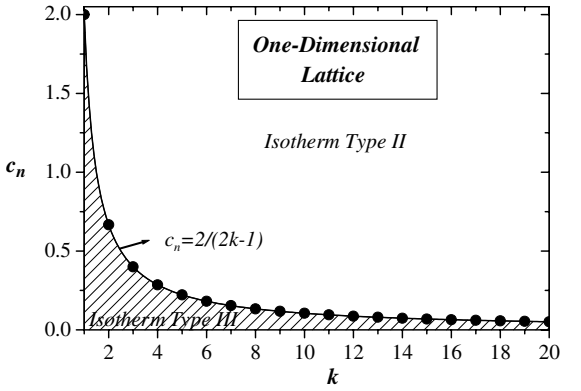

Fig. 5. c_n (as it is indicated in the text) as a function of size of adsorbate, k, for adsorption isotherms of k-mers on one-dimensional lattices.

As it is well-known, the main application of BET model consists in taking an experimental isotherm in the low-pressure region and fitting values of the monolayer volume, v_m, and the parameter c, from the slope and intercept of the linearized form of the BET equation, $(p/p_0)/[v(1 - p/p_0)] = 1/(cv_m) + (c - 1)p/(cv_m p_0)$. In this context, it is of interest to study the behavior of k-mers multilayer isotherms (with $k \geqslant 2$) in the low-pressure region in comparison with BET isotherm ($k = 1$). This comparison is shown in Fig. 6 for $c = 5$, 10, 100; $k = 1$, 2, 10; and pressures ranging from $p/p_0 = 0$

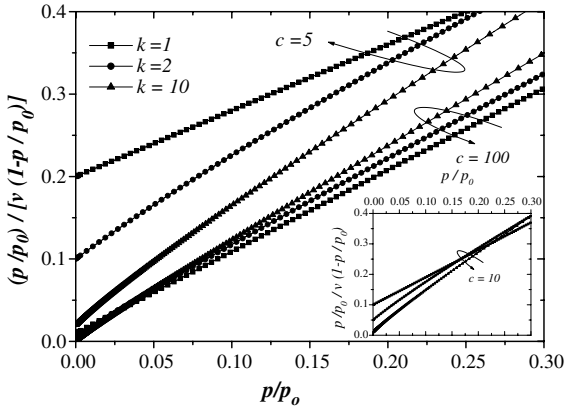

Fig. 6. $[p/p_0]/[v(1 - p/p_0)]$ versus p/p_0 for different values of c and k. All curves are plotted in the range (0–0.3) of relative pressure and v_m is set equal 1 (in arbitrary units).

up to $p/p_0 = 0.30$. A linear function is only obtained if $k = 1$. The nonlinear behavior of k-mers isotherms ($k > 1$) at low pressures, which is a distinctive characteristic of many experimental isotherms, is showing that the polyatomic character of the adsorbate must be taken into account.

The significant differences observed as k is varied indicate that the analysis of experimental isotherms of larger molecules by means of the k-mers isotherm [Eqs. (7) and (21)] would lead to values of the parameters c and v_m appreciably different from the BET ones. This effect will be widely discussed in Section 4.3.

4.2. Approximated solution in 2-D

As it is well-known, from an analytical point of view, the problem in which a two-dimensional lattice contains isolated lattice points (vacancies) as well as k-mers (with $k > 1$) has not been solved in a closed form. However, different approximate methods have been developed to study this topic. Among them, the Occupation Balance approach (OB) [28] is one of the most accurate approximation to this problem. In the simplest case of $k = 2$, the monolayer isotherm for noninteracting dimers adsorbed on a honeycomb lattice can be written as,

$$\lambda_{\mathrm{mon}}^{-1} = \frac{3}{\theta_{\mathrm{mon}}} - 5 + \frac{4}{3}\theta_{\mathrm{mon}} + \frac{2}{3}\theta_{\mathrm{mon}}^2 \quad \text{(honeycomb lattice)}. \tag{24}$$

For other connectivities, the adsorption isotherms result,

$$\lambda_{\mathrm{mon}}^{-1} = \frac{4}{\theta_{\mathrm{mon}}} - 7 + \frac{9}{4}\theta_{\mathrm{mon}} + \frac{3}{4}\theta_{\mathrm{mon}}^2 \quad \text{(square lattice)}, \tag{25}$$

$$\lambda_{\mathrm{mon}}^{-1} = \frac{6}{\theta_{\mathrm{mon}}} - 11 + \frac{23}{6}\theta_{\mathrm{mon}} + \frac{7}{6}\theta_{\mathrm{mon}}^2 \quad \text{(triangular lattice)}. \tag{26}$$

The relative pressures for honeycomb, square and triangular lattices are obtained inserting Eqs. (24)–(26), respectively, into Eq. (4). On doing so, we obtain

$$\frac{p}{p_0} = \frac{3\theta_{\mathrm{mon}}}{9c + (3 - 15c)\theta_{\mathrm{mon}} + 4c\theta_{\mathrm{mon}}^2 + 2c\theta_{\mathrm{mon}}^3} \quad \text{(honeycomb lattice)}, \tag{27}$$

$$\frac{p}{p_0} = \frac{4\theta_{\mathrm{mon}}}{16c + (4 - 28c)\theta_{\mathrm{mon}} + 9c\theta_{\mathrm{mon}}^2 + 3c\theta_{\mathrm{mon}}^3} \quad \text{(square lattice)}, \tag{28}$$

$$\frac{p}{p_0} = \frac{6\theta_{\mathrm{mon}}}{36c + (6 - 66c)\theta_{\mathrm{mon}} + 23c\theta_{\mathrm{mon}}^2 + 7c\theta_{\mathrm{mon}}^3} \quad \text{(triangular lattice)}. \tag{29}$$

The set of Eqs. (27)–(29) and Eq. (7) provide a theoretical solution to study multilayer adsorption of dimers on two-dimensional lattices. This treatment, in which the entropic effects of the adsorbate size are accounted for, bears theoretical interest because it represents a qualitative advance with respect to the existing models of multilayer adsorption.

In order to extend the study to adsorbates larger than dimers, we will start from EA model in Ref. [28]. In this paper, we presented a model to study adsorption of linear adsorbates on homogeneous surfaces. The model is based on exact forms for the thermodynamic functions of linear adsorbates in one dimension [Eq. (20)] and its generalization to higher dimensions. The resulting equation for the adsorption isotherm at monolayer is [26,28]:

$$\lambda_{\mathrm{mon}} = \frac{\theta_{\mathrm{mon}}}{k\eta(z,k)} \frac{\left[1 - \frac{(k-1)}{k}\theta_{\mathrm{mon}}\right]^{k-1}}{(1 - \theta_{\mathrm{mon}})^k}, \tag{30}$$

where z is the connectivity of the lattice and $\eta(z,k)$ represents the number of available configurations (per lattice site) for a k-mer at zero coverage.

By using Eq. (30) and following the scheme described in Section 2, the multilayer isotherm for k-mers adsorbed on a lattice of connectivity z results,

$$\frac{p}{p_0} = \frac{\theta_{\mathrm{mon}}\left[1 - \frac{(k-1)}{k}\theta_{\mathrm{mon}}\right]^{k-1}}{k\eta(z,k)c(1 - \theta_{\mathrm{mon}})^k + \theta_{\mathrm{mon}}\left[1 - \frac{(k-1)}{k}\theta_{\mathrm{mon}}\right]^{k-1}}. \tag{31}$$

It is easy to demonstrate that $\eta(z,k) = z/2$ for linear k-mers. Thus, Eq. (21) is recovered by putting $z = 2$ in Eq. (31).

In order to test the analytical results, in Figs. 7–9 simulated isotherms were compared to theoretical ones from Eqs. (27)–(29) and Eq. (31) for dimers and linear tetramers adsorbed on two-dimensional lattices with different values of c (= 0.1; 1; 10 and 100). The computational simulations were developed for honeycomb, square and triangular $L \times L$ lattices, with $L = 100$ and periodic boundary conditions. With this lattice size we verified that finite-size effects are negligible.

In the case of dimers, the agreement between OB (solid lines), EA (dashed lines) and simulated isotherms (full circles) is very good, OB being the most accurate for all lattices and for all values of c. The main differences between OB and EA are: (1) the larger the lattice connectivity the better OB reproduces the MC results. On contrary, EA provides exact results in the limit of $z = 2$ (one-dimensional lattice) and its accuracy diminishes as the connectivity increases. This behavior, which has been observed in previous studies of dimers adsorption at monolayer [28], has a simple explanation. Namely, EA is based on exact forms for the thermodynamic functions of linear adsorbates in one dimension and its generalization to higher

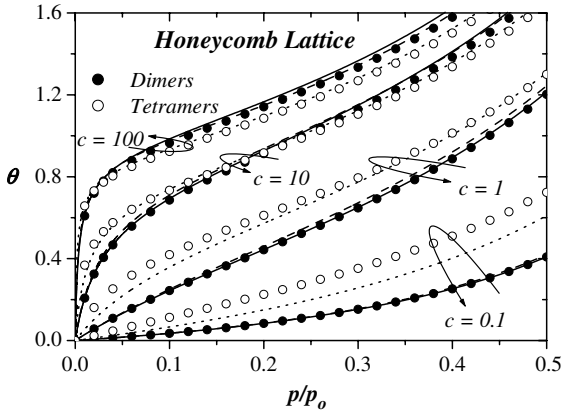

Fig. 7. Comparison between theoretical and simulated adsorption isotherms for dimers and tetramers adsorbed on honeycomb lattices with different values of the parameter c. Symbols correspond to MC simulations and lines represent theoretical results: full circles, dimers; open circles, tetramers; solid lines, data from Eq. (27); dashed lines, data from Eq. (31) (with $k = 2$ and $z = 3$); and dotted lines, data from Eq. (31) (with $k = 4$ and $z = 3$).

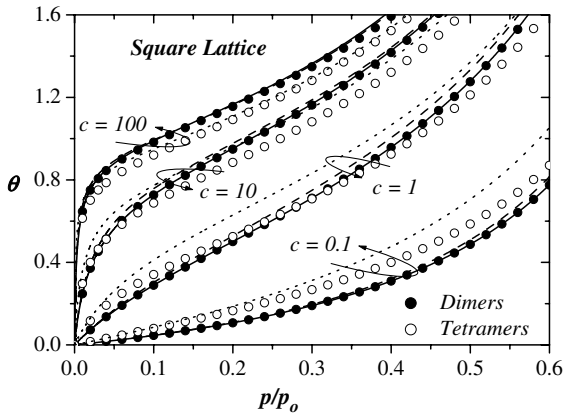

Fig. 8. Comparison between theoretical and simulated adsorption isotherms for dimers and tetramers adsorbed on square lattices with different values of the parameter c. Symbols correspond to MC simulations and lines represent theoretical results: full circles, dimers; open circles, tetramers; solid lines, data from Eq. (28); dashed lines, data from Eq. (31) (with $k = 2$ and $z = 4$); and dotted lines, data from Eq. (31) (with $k = 4$ and $z = 4$).

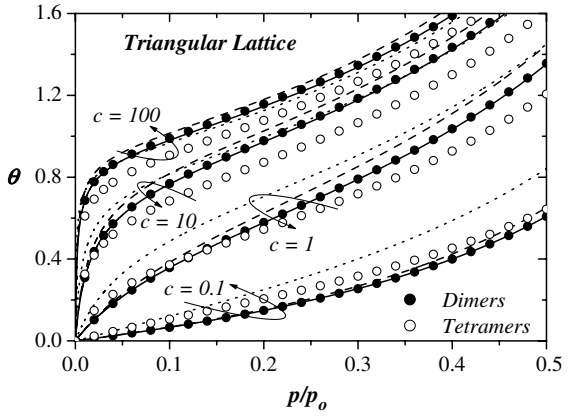

Fig. 9. Comparison between theoretical and simulated adsorption isotherms for dimers and tetramers adsorbed on triangular lattices with different values of the parameter c. Symbols correspond to MC simulations and lines represent theoretical results: full circles, dimers; open circles, tetramers; solid lines, data from Eq. (29); dashed lines, data from Eq. (31) (with $k = 2$ and $z = 6$); and dotted lines, data from Eq. (31) (with $k = 4$ and $z = 6$).

dimensions by means of a connectivity ansatz; and (2) for a given connectivity, the accuracy of OB is practically independent of c. On the other hand, EA agrees with MC results appreciably better for larger values of c.

With respect to larger adsorbates (in the particular case of Figs. 7–9, $k = 4$), the simulation results (open circles) are compared with EA isotherm Eq. (31) (dotted lines). EA model shows a qualitative agreement with MC simulations. From a quantitative point of view, the theoretical approximation agrees fairly well with the numerical results for large values of c (typically $c \approx 100$); however the disagreement turns out to be significantly large for small c's. In addition, as in the case of dimers, EA performs better for low connectivity.

Even though MC simulations of larger linear adsorbates on regular two-dimensional lattices would be necessary to confirm the applicability of Eq. (31), it should be pointed out that EA model, which is the first analytical approach for the adsorption isotherm of polyatomic molecules at multilayer, is a good one considering the complexity of the physical situation which is intended to be described.

Finally, the last goal of Figs. 7–9 is to show the effect of the spatial configuration of the molecules in the adsorbed state (depending on the surface geometry), on the multilayer adsorption properties. The phenomenon is more clearly visualized in Fig. 10, where simulated adsorption isotherms for dimers adsorbed on surfaces with different connectivities and $c = 1$, 10, 100 are plotted in part (a), and their linearized forms are shown in the range of low relative pressures in part (b). As it is observed, the lattice geometry affects appreciably the multilayer regime for weakly adsorbing surfaces ($c = 1, \ldots, 10$). It is expected that the effect increases with the adsorbate size. This effect, which is disregarded in the BET theory due to the hypothesis of independent sites, should be included in any theory treating to reproduce simulations and experiments in presence of multisite occupancy. In this sense, OB and EA represent simple and manageable analytical models for multilayer adsorption of polyatomic molecules, which are capable to account for the

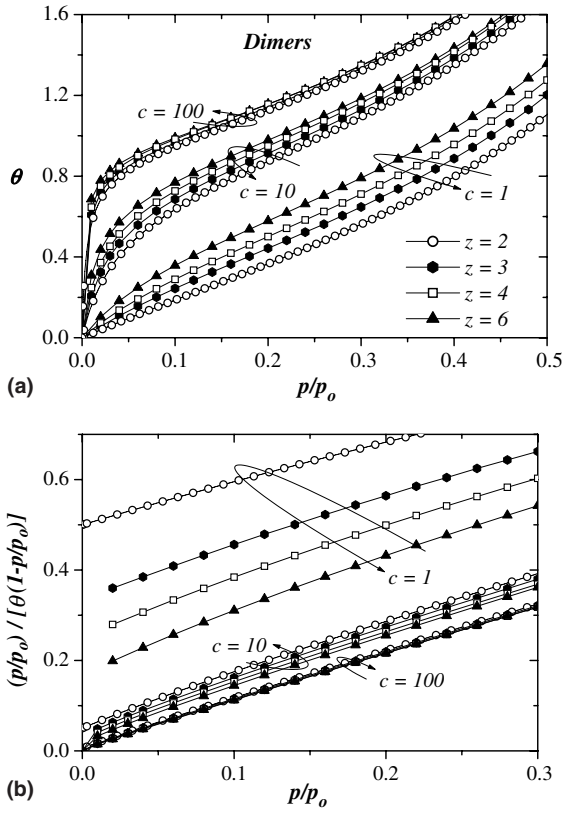

Fig. 10. (a) Simulated adsorption isotherms for dimers adsorbed on surfaces with different connectivities as indicated. In part (b), the isotherms shown in (a) are plotted in the range of low relative pressures.

structure and entropic effects of the adsorbed species.[2]

By following with the analysis about the influence of the geometry on multilayer k-mers adsorption, Fig. 11 presents the behavior of the coordinates of the point of inflection (X_F, Y_F, as in Fig. 3) for honeycomb, square and triangular adsorption isotherms of dimers with different

[2] Eq. (31) illustrates clearly the arguments above: parameter c appears along with the size of the molecule, k, and the number of available configurations (per lattice site) for a k-mer at zero coverage, $\eta(z,k)$, which is, in general, a function of the connectivity and the size of the adsorbate. Then, it is possible to define an effective parameter $c_{ef}(k,z,c) = k\eta(z,k)\ c$, which contains information about the configuration of the molecule in the adsorbed state.

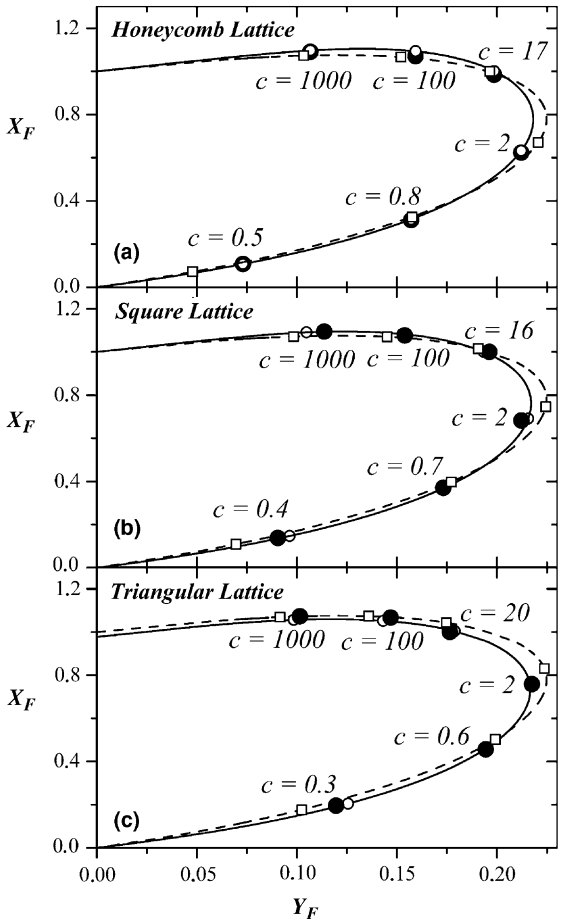

Fig. 11. Coordinates of the point of inflection (being X_F and Y_F coverage and relative pressure, respectively) for adsorption isotherms of dimers with different connectivities. Each symbol in a given curve corresponds to a determined value of c, which is indicated in the figure. Solid and dashed lines correspond to OB model and EA model, respectively, and full circles represent MC simulations results.

values of c. Solid and dashed lines correspond to OB and EA, respectively. In order to compare theoretical predictions with MC simulations (full circles), each empty circle in OB curve and each empty square in EA curve is the corresponding one to each value of c used in the simulation. The agreement between OB and computational results is excellent. In the case of EA, Eq. (31) can be rewritten as a function of c_{ef} and it is easy to demonstrate that EA predicts an universal curve (X_F, Y_F) for all connectivity. This curve reproduces fairly well the behavior of MC results at low and high values of c but quantitative differences exist for medium c's.

From the diagrams in Fig. 11, we obtained c_m and c_n as a function of z. Results are shown in Fig. 12(a) (c_m) and Fig. 12(b) (c_n). As in one-dimensional case, c_m was numerically calculated, while c_n was exactly obtained (see Appendix A). c_m decreases strongly from $z = 2$ to $z = 3$ and remains practically constant for honeycomb, square and triangular lattices. On the other hand, c_n

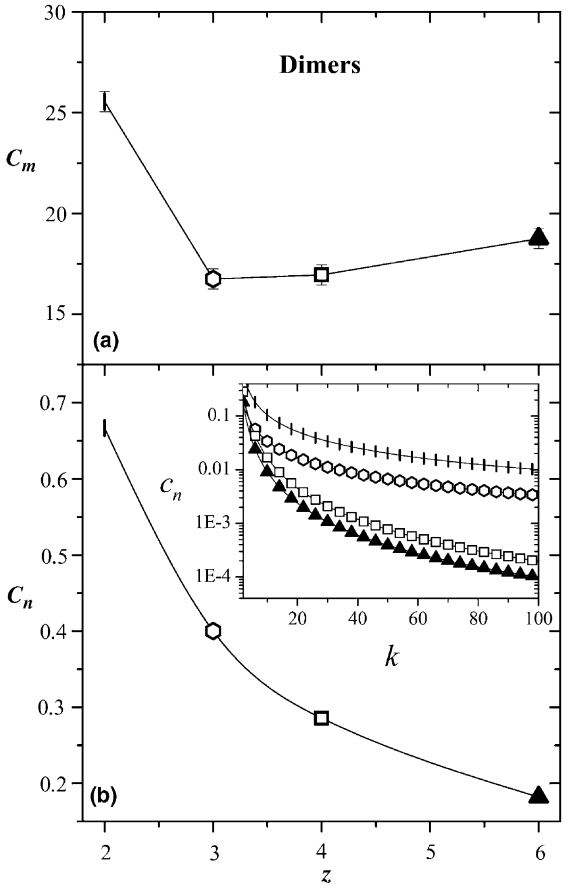

Fig. 12. (a) c_m (as it is indicated in the text) as a function of connectivity, z, for adsorption isotherms of dimers on one- and two-dimensional lattices. Symbols are as follows: vertical lines, open hexagons, open squares and full triangles represent results from one-dimensional, honeycomb, square and triangular lattices, respectively. (b) As in (a) for c_n. Inset: c_n vs. k, for one-dimensional (bars), honeycomb (hexagons), square (squares) and triangular (triangles) lattices.

decreases monotonically in the range studied. Inset in part (b) shows that this behavior continues beyond $k = 2$. In both cases, MC simulations agree very well with theoretical calculations (the data are not shown for sake of simplicity).

4.3. Comparison with experimental results

In the following, analysis of experimental results have been carried out in order to bear the significance of the adsorbate/surface geometry on the classical parameters c and v_m. For this purpose, in Fig. 13, experimental adsorption isotherms for the systems Ar [Fig. 13(a)] and N_2 [Fig. 13(b)]/nonporous silica [3], were discussed in terms of dimers isotherm equations for different connectivities [Eqs. (23), (27)–(29)]. Experimental data are reported in amount adsorbed, v [$cm^3\ g^{-1}$ (STP)], as a function of relative pressure, p/p_0. Symbols correspond to experimental data and lines represent theoretical curves. The values of the fitting parameters c and v_m are shown in Table 1. In all cases, the fitting errors do not exceed 7%. Several conclusions can be extracted from Fig. 13 and Table 1: (1) all theoretical approximations agree very well with experimental results in the range of pressure studied; (2) as in previous study [40], v_m and c resulting of the fitting from dimers isotherms differ from those corresponding with BET analysis, being $c < c_{\mathrm{BET}}$ and $v_m > v_{m,\mathrm{BET}}$; (3) v_m is not a sensitive parameter to connectivity, ranging from 38.1 ($z = 3$) to 39.9 ($z = 6$) for nitrogen and from 35.9 ($z = 3$) to 37.9 ($z = 6$) for argon; (4) c is strongly dependent on the relation adsorbate/surface geometry. The result is consistent with the definition of c as the ratio between the single-molecule partition functions in the first and higher layers. Under this consideration, c involves a mixing of energetic and entropic effects. Thus, the larger values obtained for c in the BET case trace to the compensation arising in the BET (monomer) model because of its larger entropy with respect to the dimer (k-mer) case [26]. On the other hand, the previously defined parameter c_{ef}, which contains information about the configuration of the molecule in the adsorbed state, allows us qualitatively understood the functionality of c with z (for a fixed $k = 2$). In a crude approximation, values of c in

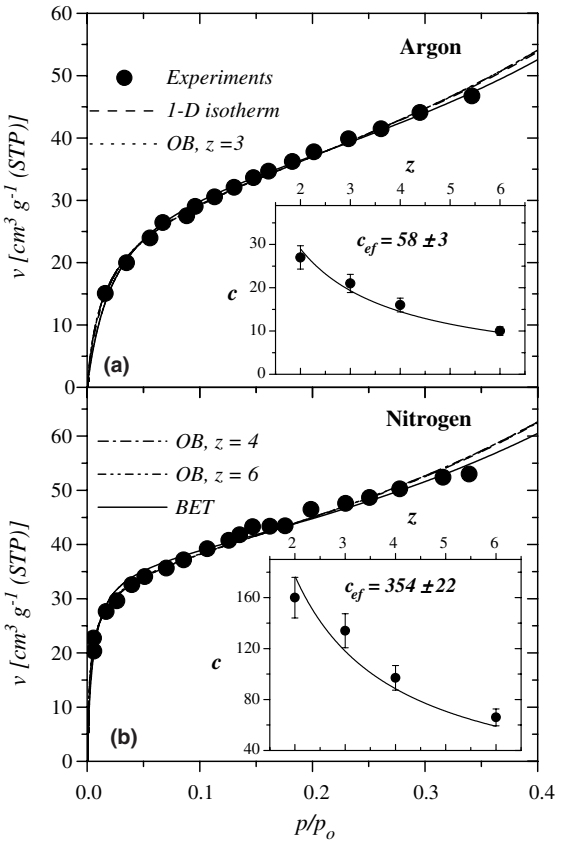

Fig. 13. Fitting of experimental adsorption isotherms of the systems Ar [part (a)] and N_2 [part (b)] on nonporous silica [3], through isotherms of dimers on 1-D [Eq. (23)] and 2-D [Eqs. (27)–(29)]. The resulting values of the parameters c and monolayer volume v_m are shown in Table 1 along with the ones arising from fitting with the BET model. Insets: (a) [(b)] Theoretical correlation of $c(z)$ (as indicated in the text) for Ar [N_2] on nonporous silica.

Table 1 can be correlated by fitting c_{ef} in function $c_{\mathrm{ef}}(k, z, c) = k\eta(z, k)c(z)$. The procedure (see insets) provides the monotonous decreasing observed in Table 1 for c [$c(z) = c_{\mathrm{ef}}/z$], where the values obtained for c_{ef} were (354 ± 22) and (58 ± 3) for nitrogen and argon, respectively.

In Fig. 14, linearized forms of isotherms in Fig. 13 are plotted in the range of low pressure. By using the same fitting parameters of Table 1, experimental data are compared with theoretical curves. In all cases, theoretical isotherms provide very good approximations. As in many experimental isotherms, a detailed analysis of theoretical

Table 1
Resulting values of the parameters c and monolayer volume v_m from fitting in Figs. 13 and 14

Adsorbate/nonporous silica	1-D, Eq. (23)		OB, $z = 3$		OB, $z = 4$		OB, $z = 6$		BET	
	c	v_m	c	v_m	c	v_m	c	v_m	c	v_m
N_2	160	39.0	134	38.1	97	38.7	66	39.9	206	36.5
Ar	27	36.5	21	35.9	16	36.5	10	37.9	43	32.5

v_m is expressed in $cm^3\ g^{-1}$ (STP).

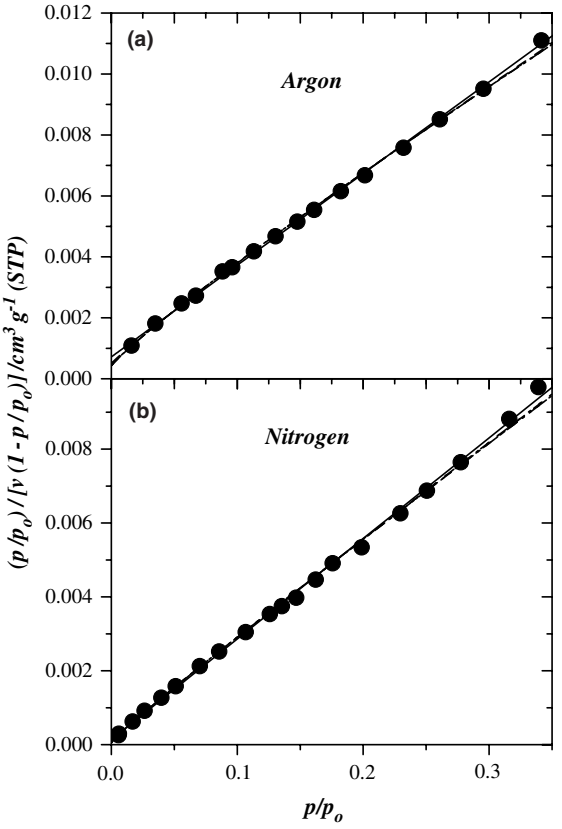

Fig. 14. Low-pressure adsorption data of Ar [part (a)] and N_2 [part (b)] on nonporous silica, complete data given in Fig. 13.

data indicates a nonlinear behavior of Eqs. (23) and (27)–(29) at low pressure. In other words, the rigorous treatment of multilayer adsorption considering the polyatomic nature of the adsorbate, is indicating that multisite occupancy is a source of nonlinearity, even though lateral interactions and surface heterogeneity are not accounted for in the model.

5. Conclusions

In the present paper, an analytical approach to the multilayer adsorption isotherm of polyatomic adsorbates (k-mers) has been proposed. The approximation provides the isotherm in the multilayer regime from the isotherm at monolayer. In this framework, exact solution in one dimension was obtained and calculations were extended to k-mers in two-dimensional surfaces, based upon the OB and EA approximations [28].

The proposed model is simple, easy to apply in practice, and leads to new values of surface area and adsorption heats. Physically, these advantages are a consequence of properly considering the configurational entropy of the adsorbate. This treatment, in which the entropic effects of the adsorbate size are accounted for, bears theoretical interest because it represents a qualitative advance with respect to the existing models of multilayer adsorption.

In all cases, theoretical predictions were discussed and compared with MC simulated data, which reinforces the robustness of the two methodologies employed here.

In addition, experimental adsorption isotherms of argon and nitrogen on nonporous silica have been adjusted in order to test the applicability of our theoretical model. Several conclusions can be drawn from the fitting of experimental data. On one hand, the monolayer volume (or equivalently, surface area), v_m, resulting from experiments by using the one-dimensional isotherm of dimers (i) is approximately 1.1 times the corresponding ones from BET; and (ii) remains practically constant with increasing connectivity and $k = 2$. On the other hand, the parameter c depends on size of adsorbate and connectivity. In this sense, our goal was to develop a simple model for $c(z)$, which was

capable to reproduce the correct qualitative behavior of the fitting values for c from multilayer isotherm equations for different connectivities.

In summary, an important advance has been addressed in the present contribution by including, in a very simple way, the effect of the adsorbate/surface geometry on the multilayer adsorption theory. This effect, which is not taking into account in the standard BET model, should be very important in numerous real systems in presence of multisite occupancy.

Acknowledgments

This work was supported in part by CONICET (Argentina) under project PIP 02425 and the Universidad Nacional de San Luis (Argentina) under the projects 328501 and 322000. One of the authors (A.J.R.P.) is grateful to the Departamento de Química, Universidad Autónoma Metropolitana-Iztapalapa (México, D.F.) for its hospitality during the time this manuscript was prepared.

Appendix A

In order to determine c_n, we calculate the inflection point of the adsorption isotherm

$$\frac{\mathrm{d}^2\theta}{\mathrm{d}(p/p_0)^2} = 0 \quad \text{and} \quad p/p_0 \to 0 \quad \text{(low density)}. \tag{32}$$

By calculating the second derivative of θ in Eq. (7), we obtain:

$$\theta'' = \frac{\theta''_{\mathrm{mon}}}{(1-p/p_0)} + \frac{2\theta'_{\mathrm{mon}}}{(1-p/p_0)^2} + \frac{2\theta_{\mathrm{mon}}}{(1-p/p_0)^3}, \tag{33}$$

where θ'' and θ' represent $\partial\theta/\partial(p/p_0)$ and $\partial^2\theta/\partial(p/p_0)^2$, respectively. Now, by taking $\lim_{p/p_0\to 0}$ in Eq. (33), which implies $\lim_{\theta_{\mathrm{mon}}\to 0}$, the following relation is obtained:

$$0 = \theta''_{\mathrm{mon}} + 2\theta'_{\mathrm{mon}}. \tag{34}$$

The last equation allows us to obtain c_n from the monolayer adsorption isotherm. At low density ($\theta_{\mathrm{mon}} \to 0$), the Occupation Balance approach can be considered as an exact result [28]. In general, the monolayer adsorption isotherm can be written as:

$$\frac{1}{\lambda} = \frac{R}{n}, \tag{35}$$

where R is the mean number of states available to the $(n+1)$th molecule, given n particles already adsorbed on a lattice of M sites. R can be written as:

$$R = G - gn + nf(\theta_{\mathrm{mon}}). \tag{36}$$

G (g) represents the number of equilibrium states available to a single molecule (the number of states excluded per molecule) at infinitely low density. Due to the number of states excluded per molecule depends in general on the number of molecules n in the surface, a correction function, $f(\theta_{\mathrm{mon}})$, is introduced. For instance, $G = M$, $g = 1$ and $f = 0$ for monomers. On the other hand, $G = 2M$, $g = 7$ and $f \neq 0$ [28] for dimers adsorbed on a square lattice of M sites. We propose that $f(\theta_{\mathrm{mon}})$ can be expanded in a power series in terms of θ_{mon}:

$$f(\theta_{\mathrm{mon}}) = \sum_{i=1}^{\infty} a_i \theta_{\mathrm{mon}}^i. \tag{37}$$

The inverse of the fugacity can be determined from Eqs. (35) and (36),

$$\frac{1}{\lambda} = \frac{G}{n} - g + f(\theta_{\mathrm{mon}}). \tag{38}$$

Then, by using Eq. (37) and Eq. (4), the relative pressure can be written as:

$$p/p_0 = \frac{\theta_{\mathrm{mon}}}{cG_k + (1-cg)\theta_{\mathrm{mon}} + c\theta_{\mathrm{mon}} f(\theta_{\mathrm{mon}})} = \frac{\theta_{\mathrm{mon}}}{F(\theta_{\mathrm{mon}})}, \tag{39}$$

where $G_k = kG/M$. Differentiating both sides of Eq. (39) with respect to p/p_0, we obtain:

$$1 = \frac{\theta'_{\mathrm{mon}} F(\theta_{\mathrm{mon}}) - \theta_{\mathrm{mon}} F'(\theta_{\mathrm{mon}})}{F^2(\theta_{\mathrm{mon}})}. \tag{40}$$

By taking $\theta_{\mathrm{mon}} \to 0$ in Eq. (40), we arrive to the expression:

$$\theta'_{\mathrm{mon}} = c_n G_k. \tag{41}$$

Differentiating again Eq. (40) with respect to p/p_0, and using simple algebraic operations, we obtain:

$$\theta'_{\mathrm{mon}} = 2c_n G_k(1 - c_n g). \tag{42}$$

Finally, from Eqs. (34), (41) and (42), which are valid only in the limit $p/p_0 \to 0$, we can determine the value of c_n:

$$c_n = \frac{2}{g}. \tag{43}$$

As it can be observed, the expansion coefficients in Eq. (37) do not appear in Eq. (43). Consequently, Eq. (43) is exact. For the one-dimensional case $g = 2k - 1$, which implies

$$c_n = \frac{2}{2k-1}. \tag{44}$$

Eq. (44) is valid for $k \geqslant 1$ ($c_n = 2$ for monomers). On the other hand, for two-dimensional lattices:

$$g = \begin{cases} 5 & \text{for } k = 2, \\ 6k - 1 & \text{for } k > 2 \quad \text{honeycomb lattices,} \end{cases} \tag{45}$$

then

$$c_n = \begin{cases} \frac{2}{5} & \text{for } k = 2, \\ \frac{2}{6k-1} & \text{for } k > 2 \quad \text{honeycomb lattices,} \end{cases} \tag{46}$$

$$g = k^2 + 2k - 1 \quad \text{for } k \geqslant 2 \quad \text{square lattices,} \tag{47}$$

then

$$c_n = \frac{2}{k^2 + 2k - 1} \quad \text{for } k \geqslant 2 \quad \text{square lattices,} \tag{48}$$

$$g = 2k^2 + 2k - 1 \quad \text{for } k \geqslant 2 \quad \text{triangular lattices,} \tag{49}$$

then

$$c_n = \frac{2}{2k^2 + 2k - 1} \quad \text{for } k \geqslant 2 \quad \text{triangular lattices.} \tag{50}$$

References

[1] A. Clark, The Theory of Adsorption and Catalysis, Academic Press, New York, 1970.

[2] W.A. Steele, The Interaction of Gases with Solid Surfaces, Pergamon Press, New York, 1974.

[3] S.J. Gregg, K.S.W. Sing, Adsorption, Surface Area, and Porosity, Academic Press, New York, 1991.

[4] A.W. Adamson, Physical Chemistry of Surfaces, John Wiley and Sons, New York, 1990.

[5] J. Frenkel, Kinetic theory of liquids, Clarendon Press, Oxford, 1946;
J. Frenkel, Kinetic Theory of Liquids, Dover Reprint, New York, 1955.

[6] G.D. Halsey, J. Chem. Phys. 16 (1948) 931.

[7] T.L. Hill, Adv. Catal. 4 (1952) 211.

[8] W.G. McMillan, E. Teller, J. Chem. Phys. 19 (1951) 25;
W.G. McMillan, E. Teller, J. Phys. Colloid Chem. 55 (1951) 17.

[9] S. Brunauer, P.H. Emmet, E. Teller, J. Am. Chem. Soc. 60 (1938) 309.

[10] W. Rudzinski, D. Everett, Adsorption of Gases on Heterogeneous Surfaces, Academic Press, New York, 1992.

[11] P. Zeppenfeld, J. George, V. Diercks, R. Halmer, R. David, G. Cosma, A. Marmier, C. Ramseyer, C. Girardet, Phys. Rev. Lett. 78 (1997) 1504.

[12] O.G. Mouritsen, A.J. Berlinsky, Phys. Rev. Lett. 48 (1982) 181.

[13] D. Ferry, J. Suzanne, Surf. Sci. 345 (1996) L19.

[14] J.W. He, C.A. Estrada, J.S. Corneille, M.C. Wu, D.W. Goodman, Surf. Sci. 261 (1992) 164.

[15] V. Panella, J. Suzanne, P.N.M. Hoang, C. Girardet, J. Phys. I 4 (1994) 905.

[16] D.L. Meixner, D.A. Arthur, S.M. George, Surf. Sci. 261 (1992) 141.

[17] C. Pierce, B. Ewing, J. Phys. Chem. 68 (1964) 2562.

[18] E.A. DiMarzio, J. Chem. Phys. 35 (1961) 658.

[19] T. Nitta, M. Kuro-Oka, K. Katayama, J. Chem. Eng. Jpn. 17 (1984) 45.

[20] W. Rudziński, K. Nieszporek, J.M. Cases, L.I. Michot, F. Villeras, Langmuir 12 (1996) 170.

[21] J.-H. Ryu, P.D. Gujrati, J. Chem. Phys. 107 (1997) 3954.

[22] P.D. Gujrati, J. Chem. Phys. 108 (1998) 5089.

[23] D.-W. Wu, G.L. Aranovich, M.D. Donohue, J. Colloid Interf. Sci. 230 (2000) 281.

[24] G.L. Aranovich, M.D. Donohue, J. Colloid Interf. Sci. 213 (1999) 457.

[25] D.-W. Wu, G.L. Aranovich, M.D. Donohue, J. Colloid Interf. Sci. 212 (1999) 301.

[26] A.J. Ramirez-Pastor, T.P. Eggarter, V.D. Pereyra, J.L. Riccardo, Phys. Rev. B 59 (1999) 11027.

[27] A.J. Ramirez-Pastor, A. Aligia, F. Romá, J.L. Riccardo, Langmuir 16 (2000) 5100.

[28] F. Romá, A.J. Ramirez-Pastor, J.L. Riccardo, Langmuir 19 (2003) 6770.

[29] J.L. Riccardo, A.J. Ramirez-Pastor, F. Romá, Phys. Rev. Lett. 93 (2004) 186101.

[30] M. Borówko, W. Rżysko, J. Colloid Interf. Sci. 82 (1996) 268;
M. Borówko, W. Rżysko, Ber. Bunsenges. Phys. Chem. 101 (1997) 84.

[31] W. Rżysko, M. Borówko, J. Chem. Phys. 117 (2002) 4526;
W. Rżysko, M. Borówko, Surf. Sci. 520 (2002) 151.
[32] A.J. Ramirez-Pastor, M.S. Nazzarro, J.L. Riccardo, G. Zgrablich, Surf. Sci. 341 (1995) 249.
[33] A.J. Ramirez-Pastor, M.S. Nazzarro, J.L. Riccardo, V. Pereyra, Surf. Sci. 391 (1997) 267.
[34] A.J. Ramirez-Pastor, J.L. Riccardo, V. Pereyra, Surf. Sci. 411 (1998) 294.
[35] A.J. Ramirez-Pastor, J.L. Riccardo, V.D. Pereyra, Langmuir 16 (2000) 10167.
[36] J.E. González, A.J. Ramirez-Pastor, V.D. Pereyra, Langmuir 17 (2001) 6974.
[37] F. Romá, A.J. Ramirez-Pastor, J.L. Riccardo, J. Chem. Phys. 114 (2001) 10932.
[38] G.L. Aranovich, M.D. Donohue, J. Colloid Interf. Sci. 175 (1995) 492.
[39] G.L. Aranovich, M.D. Donohue, J. Colloid Interf. Sci. 189 (1997) 101.
[40] J.L. Riccardo, A.J. Ramirez-Pastor, F. Romá, Langmuir 18 (2002) 2130.
[41] N. Metropolis, A.W. Rosenbluth, M.N. Rosenbluth, A.H. Teller, E. Teller, J. Chem. Phys. 21 (1953) 1087.